Short communication

Effect of Al$_2$O$_3$ coating on electrochemical performance of LiCoO$_2$ as cathode materials for secondary lithium batteries

Seungsuk Oh [a], Joong Kee Lee [b,*], Dongim Byun [a], Won Ii Cho [b], Byung Won Cho [b]

[a] *Department of Materials Science & Engineering, Korea University, Seoul 136-701, South Korea*
[b] *Eco-Nano Research Center; KIST, Seoul 130-650, South Korea*

Abstract

Al$_2$O$_3$-coated LiCoO$_2$ particles are prepared by a gas-suspension spray method with coatings in the range from 0.1 to 2.0 wt.%, and are examined for their electrochemical performance with special attention to the surface coverage of cathode materials for lithium-ion batteries. The Al$_2$O$_3$ coating increases both the surface area and the electrical conductivity of LiCoO$_2$, improves the cycle performance even at a higher cut-off charge voltage, and induces higher thermal stability. In the experimental range studied, different coating amounts (i.e., surface coverage of Al$_2$O$_3$) causes different capacity retention after 50 cycles. The optimum Al$_2$O$_3$ coating amount for the highest capacity retention is 0.2 wt.%. This corresponds to 13.7% of surface coverage.
© 2004 Elsevier B.V. All rights reserved.

1. Introduction

LiCoO$_2$ has been commercially employed as an active material for the cathode of lithium-ion batteries because of its good rate capability and stable capacity [1–4]. LiCoO$_2$ has a layered-type (rhombohedral) structure with R3m symmetry. The lithium and cobalt ions occupy alternate octahedral sites between the cubic-close-packed oxygen planes. Thus, lithium ions de-intercalate and intercalate during the charge–discharge process. LiCoO$_2$ is stable when cycled from the fully-lithiated discharge state viz., LiCoO$_2$ (3.8 V versus Li) to the half-delithiated charge state viz., Li$_{0.5}$CoO$_2$ (4.2 V versus Li) [5]. Its capacity fades rapidly, however, when more Li ions are extracted from the lattice [6,7]. LiCoO$_2$ loses lithium ions and electrons during the charge process. During de-intercalation of Li ions, Co^{3+} is oxidized to unstable Co^{4+} and is dissolved in the electrolyte. Therefore, increase in the Co^{4+} concentration will damage the cathode crystal. Contraction along the c axis results in mechanical failure of the LiCoO$_2$ particles and rapid capacity fading [8]. Many studies have been carried out to improve the structure stability of LiCoO$_2$ [9–12]. Modification of the surface properties of the cathode materials by coating with some metal oxides has been recognized as

one of the most reliable techniques [13–15]. The advantage of this technique is that side reactions on the surface with electrolyte are avoided and structural breakage of LiCoO$_2$ during charge–discharge cycling can be moderated.

In this study, Al$_2$O$_3$ is coated on the surface of LiCoO$_2$ particles by a gas-suspension spray coating method and the effect of the coating on the structural and cycle stabilities of LiCoO$_2$ cathode are investigated.

2. Experimental

Commercial LiCoO$_2$ powder (Nippon Chemical Industry) was used as the raw material for Al$_2$O$_3$ coating. The average particle size of LiCoO$_2$, as determined by a centrifugal particle size distribution analyzer, was 7.7 μm. Al$_2$O$_3$-coated LiCoO$_2$ was prepared by a gas-suspension spray coating method. The coating solution, was aluminum lactate dissolved into a mixture of distilled water and ethanol. LiCoO$_2$ powders were suspended by a fluidizing gas in a reactor and were wetted by the atomized coating solution that was sprayed through a nozzle which was placed at the bottom of the container. The wetted powders were extensively dried through solvent evaporation at 80 °C. The repeated motion of the powders through the spray zone allowed a continuous coating of material to build up and, finally, uniform coating powders could be prepared. The amount of
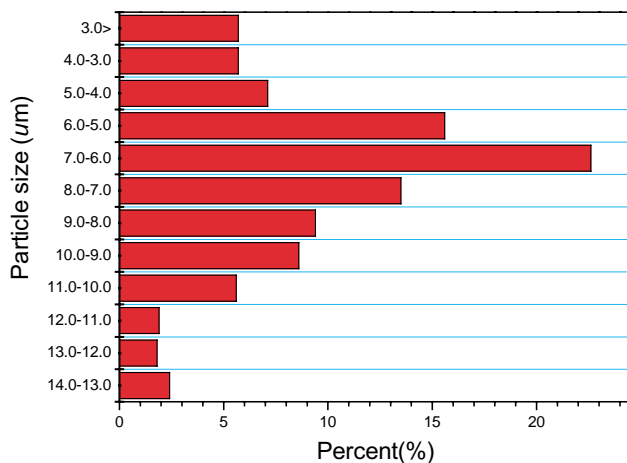
Fig. 1. Particle-size distribution of LiCoO$_2$ particles.

Al_2O_3 coated on the LiCoO$_2$ could be controlled from 0.1 to 2 wt.% by adjusting the spraying time. The LiCoO$_2$ powders coated with metal solution were calcined in a furnace at 300 °C for 3 h and at 500 °C for 3 h under an oxygen atmosphere. Al_2O_3-coated LiCoO$_2$ was mixed with acetylene black (AB) to provide a conductor, and with a PVDF binder at a weight ratio of Al_2O_3-coated LiCoO$_2$:AB:binder = 85:9:6 in acetone to prepare a slurry. The slurry was spread on aluminum foil by a dipping method to make the positive electrode. The resulting electrode sheets were dried in a vacuum oven at 80 °C for more than 24 h for later use. Half-cells were assembled in a dry room with LiCoO$_2$ as the working electrode, lithium foil as the counter electrode, 1 M LiPF$_6$ in ethylene carbonate (EC):demiethyl carbonate (DMC):ethylmethyl carbonate (EMC) 1:1:1 by volume %) as the electrolyte, and a polypropylene-based film as the separator.
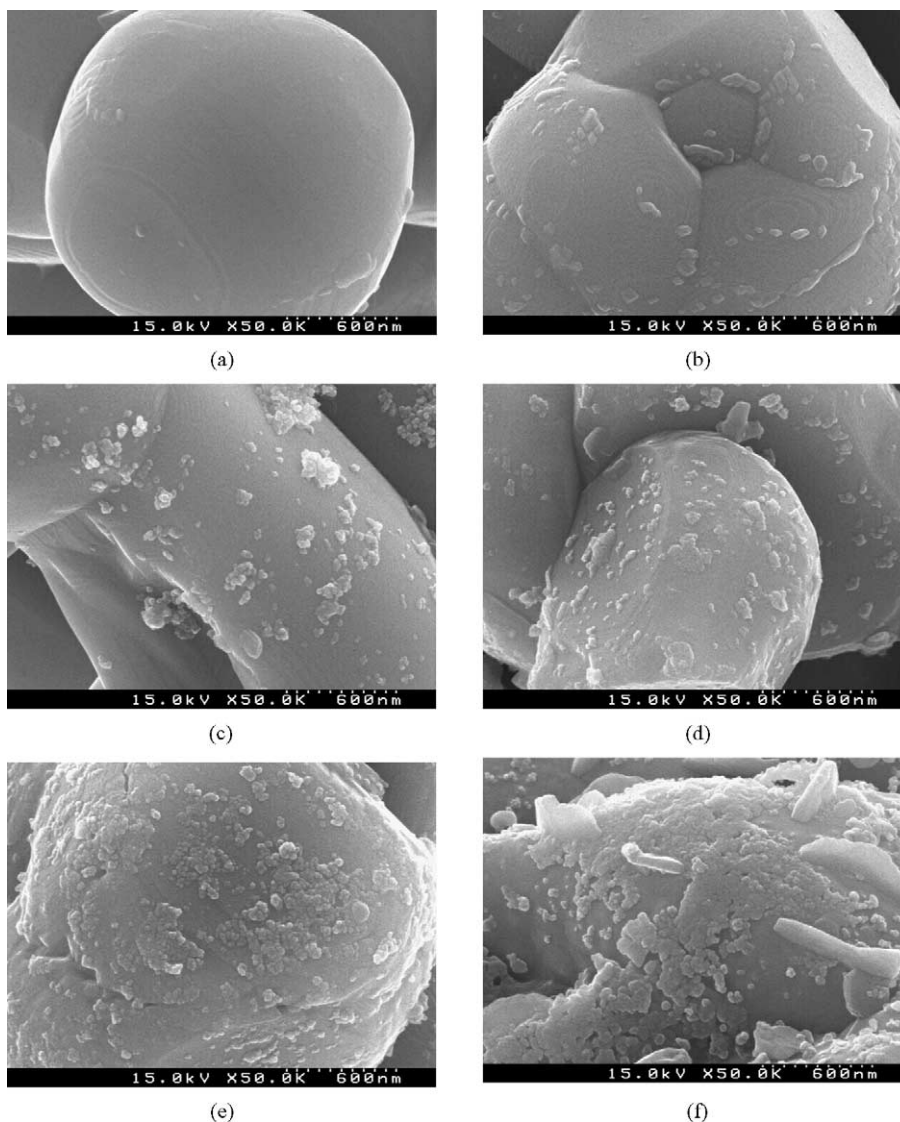

Fig. 2. Scanning electron micrographs of bare LiCoO$_2$ and Al_2O_3-coated LiCoO$_2$, (a) bare LiCoO$_2$; (b)Al_2O_3, 0.1 wt.% coated; (c) Al_2O_3, 0.2 wt.% coated; (d) Al_2O_3, 0.5 wt.% coated; (e) Al_2O_3, 1 wt.% coated; (f) Al_2O_3, 2 wt.% coated LiCoO$_2$.
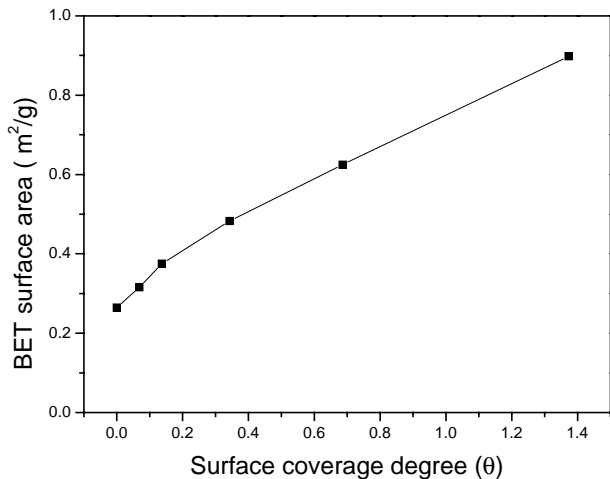
Fig. 3. BET surface area of Al_2O_3-coated $LiCoO_2$ with various degrees of surface coverage.

The Al_2O_3-coated $LiCoO_2$ powders, were characterized in terms of:

(i) Surface morphology by means of a scanning electron microscope (SEM: Hitachi S-4200);
(ii) specific surface area by the BET method (ASAP: Micromeritics ASAP-2010);
(iii) conductivity by electrical resistivity measurements;
(iv) depth profile by Auger electron spectroscopy (AES);
(v) cobalt content in the electrolyte by an atomic absorption spectrophotometer(AAS).

Charge–discharge cycling tests were performed with computer-controlled, multi-channel, battery test units (Won A Tech WBC3000) at the 0.2 C rate between 3.0 V and two different charge cut-off voltages of 4.2 and 4.4 V. Differential scanning calorimetry (DSC: Perkin-Elmer Pyris1) experiments were carried out after charging test cells at
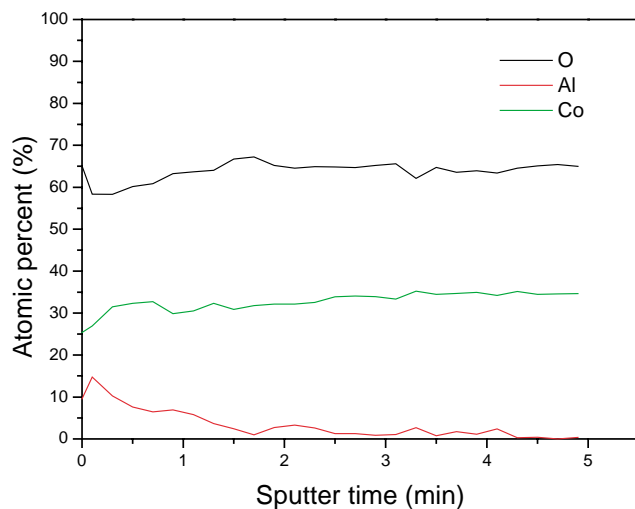
Table 1
AAS analysis of dissolved Co content of bare and Al_2O_3-coated $LiCoO_2$ immersed in 1 M $LiPF_6$-EC:DMC:EMC (l:1:1) electrolyte

Sample	Co content dissolved in electrolyte (mg l^{-1})
Bare $LiCoO_2$	3.10
Al_2O_3 0.2 wt.% coated $LiCoO_2$	1.32

4.2 V. For DSC experiments, cells were charged to 4.2 V at the 0.2 C rate, followed by holding at the same potential for 20 h [16]. The cells were then dissembled in a dry room to obtain charged cathode samples. The heating rate of the DSC experiment was 3 °C per min.

3. Results and discussion

3.1. Characterization of Al_2O_3-coated $LiCoO_2$ particles

The particle-size distribution of $LiCoO_2$ is shown in Fig. 1. The density of $LiCoO_2$ measured by pycnometer is $4.76\,g\,cm^{-3}$ and the range of the particle size determined by the centrifugal particle-size distribution analyzer based on the density of $LiCoO_2$ is from 3 to 14 μm. Also, the observed average particle diameter of $LiCoO_2$ is 7.7 μm, as shown in Fig. 1. Scanning electron micrographs for bare and Al_2O_3-coated $LiCoO_2$ are shown in Fig. 2. Bare $LiCoO_2$ has a very smooth surface (Fig. 2(a)). For the coated electrode, Al_2O_3 particles are deposited throughout the surface of $LiCoO_2$ (Fig. 2(b)–(f)). The surface is completely covered when a 2 wt.% Al_2O_3 coating is applied. The BET surface-area increases with the degree of surface coverage. In this work, the surface coverage is defined as the ratio of total cross-section area of Al_2O_3 to total surface of $LiCoO_2$ and θ indicates the degree of surface coverage.
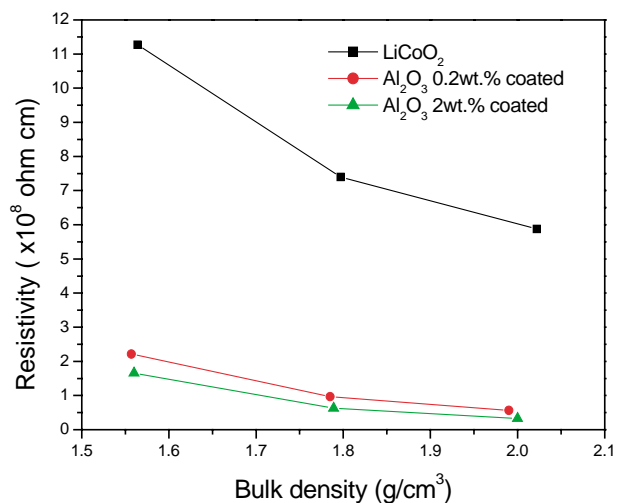

Fig. 4. Depth profile of Al_2O_3-coated $LiCoO_2$ particles determined by Auger electron spectroscopy.

Fig. 5. Volume resistivity of bare $LiCoO_2$ and Al_2O_3-coated $LiCoO_2$ determined by resistivity measurement tool.
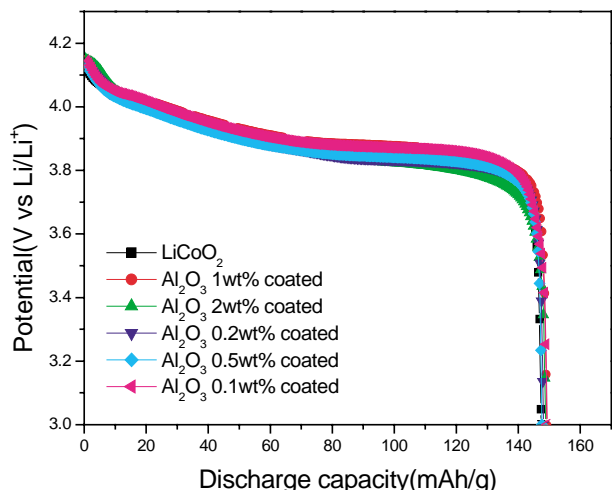
Fig. 6. Discharge curves of bare $LiCoO_2$ and Al_2O_3-coated $LiCoO_2$ on first cycle (charge: 3 to 4.2 V at 0.2 °C rate).

Fig. 8. Variation of capacity retention after 50 cycles with degree of surface coverage.

To calculate the surface coverage, the diameter of $LiCoO_2$ was defined as 7.7 μm and the diameter of Al_2O_3 was defined as 50 nm. As shown in Fig. 3, the degree of surface coverage of $LiCoO_2$ coated with 2 wt.% of Al_2O_3 is greater than unity.

The AES depth profiles of the Al_2O_3-coated $LiCoO_2$ particles at a scan rate of 10.5 nm min^{-1} are given in Fig. 4. The content of Al decreases with depth and after 1.5 min is insignificant. Therefore, the distance of diffusion of Al^{3+} ions into the $LiCoO_2$ is about 15 nm. This observation indicates that a thin layer of Li–Al–Co–O is formed on the surface of $LiCoO_2$. This thin layer protects the $LiCoO_2$ particles from dissolution in the electrolyte. An exact amount (about 30 mg) of bare and Al_2O_3-coated $LiCoO_2$ particles was immersed in 12 ml of 1 M $LiPF_6$-EC:DMC:EMC (1:1:1 by volume) electrolyte for 1 week. Then the amount of dissolved Co^{4+} in the electrolyte was quantitatively determined by atomic absorption spectroscopy (AAS) analysis. As shown in Table 1, the
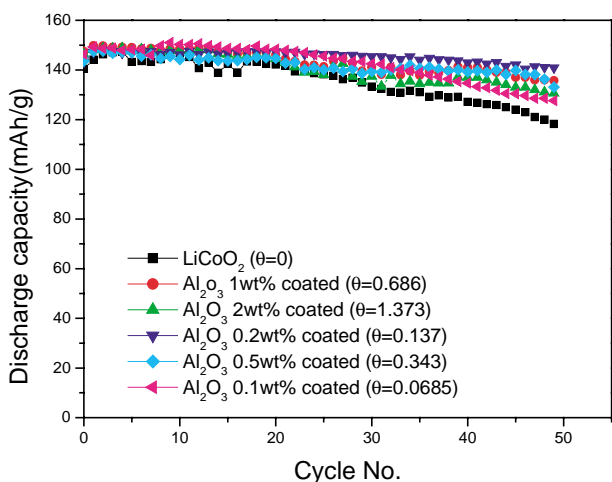
dissolved Co content of Al_2O_3-coated $LiCoO_2$ is lower than that of bare $LiCoO_2$. The data show that the Al_2O_3 coating can effectively reduce dissolution of $LiCoO_2$ into the electrolyte. This finding is in agreement with that obtained with AES depth profiles.

Therefore, the thin layer of Li–Al–Co–O on the surface of $LiCoO_2$ plays an important role in preserving the structure of the shell from the electrolyte.

The difference in the volume resistivity of bare $LiCoO_2$ and Al_2O_3-coated $LiCoO_2$ as determined by using a resistivity measurement tool, is shown in Fig. 5. The dimensions of the resistivity measurement tool have been reported in detail in a previous study [17]. The amount of Al_2O_3 coating on the samples was 0.2 and 2 wt.%. The volume resistivity can be calculated by measurement of the potential drop between two probes at various currents. The results in Fig. 5 indicate that the volume resistivities of the two Al_2O_3-coated

Fig. 7. Cycling performance of bare $LiCoO_2$ and Al_2O_3-coated $LiCoO_2$. (charge: 3 to 4.2 V at 0.2 °C rate).

Fig. 9. Cycling performance of bare $LiCoO_2$ and Al_2O_3-coated $LiCoO_2$. (charge: 3 to 4.4 V at 0.2 °C rate).

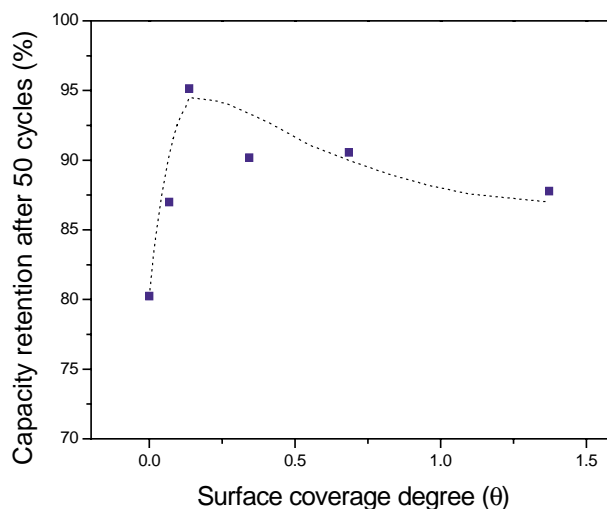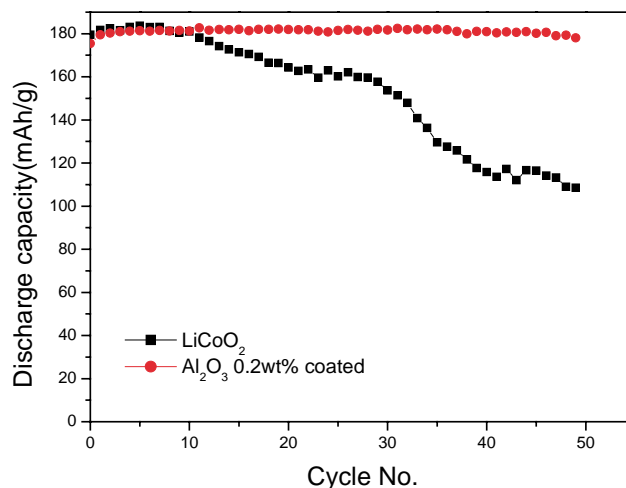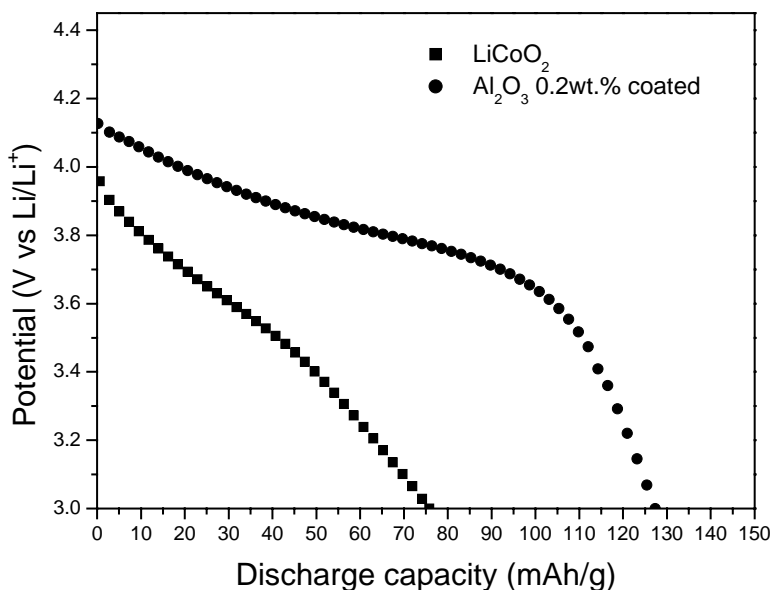Fig. 10. Comparison of thermal stability cells using bare LiCoO$_2$ and Al$_2$O$_3$-coated LiCoO$_2$. Cells charged to 4.4 V at 0.2 °C rate, and then held at this potential for 20 h. Before measurement of discharge capacity, the cells were placed in an oven at 90 °C for 4 h.

LiCoO$_2$ samples are lower than that of bare LiCoO$_2$. Given that Al$_2$O$_3$ has a lower electrical conductivity than LiCoO$_2$, it was expected that the Al$_2$O$_3$ coating on the surface of the LiCoO$_2$ particles would not enhance the conductivity [18]. The actual observed increase in electrical conductivity caused by the Al$_2$O$_3$ coating is therefore probably due to an Al$_2$O$_3$ doping effect in the matrix of the LiCoO$_2$ surface.

3.2. Electrochemical performance

Discharge–potential curves for the first cycle of bare and Al$_2$O$_3$-coated LiCoO2 with different coating amounts are shown in Fig. 6. The cell voltage was changed from 4.2 to 3 V at the 0.2 C charge–discharge rate. The difference in discharge capacities between bare LiCoO$_2$ and Al$_2$O$_3$-coated LiCoO$_2$ is very small.

The change in discharge capacities with repeated charge–discharge cycles for bare and Al$_2$O$_3$-coated LiCoO$_2$ with various coating amounts presented in Fig. 7. The cell voltage was charged from 4.2 to 3 V at the 0.2 C charge–discharge rate. For all of the samples, the discharge capacities decrease slowly with cycling, possibly due to a structural change in the LiCoO$_2$ crystal lattice. The discharge capacity of bare LiCoO$_2$ decreases to 80% of initial capacity. By contrast, the 0.2 wt.% Al$_2$O$_3$-coated LiCoO$_2$ maintains its initial capacity at over 95%, even after 50 cycles. As shown in Fig. 7 the capacity retention after 50 cycles generally decreases with increase in the degree of surface coverage degree (θ). These results indicate that existence of even a small coating of Al$_2$O$_3$ increases the structural stability of LiCoO$_2$ during charge–discharge cycling. As mentioned before, Al^{3+} ions diffuse into the

LiCoO$_2$ and from the thin layer at the surface LiCoO$_2$. The sites for Al^{3+} are, however, limited. Therefore, an excess of Al^{3+} ions hinders the extraction and insertion of Li ions from/into the LiCoO$_2$ [19] and twist the structure of LiCoO$_2$ [20]. The data in Fig. 8 indicate that 0.2 wt.% Al$_2$O$_3$-coated LiCoO$_2$, which corresponds to a surface coverage degree of 0.137, is the best level for providing high cycling performance, and that greater coating amounts do not produce any further enhancement.

A comparison of the cycleability of bare and 0.2 wt.% Al$_2$O$_3$-coated LiCoO$_2$ in the higher voltage range is given in Fig. 9. The cell voltage was changed from 4.4 to 3 V at 0.2 C rate. The capacity retention after 50 cycles for bare and the surface-modified LiCoO$_2$ is 59.01 and 97.51%, respectively. The effect of Al$_2$O$_3$ coating on cycleability is obvious in the higher voltage range.

3.3. Thermal stability of Al$_2$O$_3$-coated LiCoO$_2$

The thermal stability of bare and 0.2 wt.% Al$_2$O$_3$-coated LiCoO$_2$ is given in Fig. 10. The test half-cells were charge to 4.4 V and then held at this potential for 20 h. After the test cells were placed in an oven at 90 °C for 4 h, the discharge capacities were measured. The discharge capacity of 0.2 wt.% Al$_2$O$_3$-coated LiCoO$_2$ is 125 mAh g^{-1}. By contrast, the capacity of bare LiCoO$_2$ decreases sharply to 75 mAh g^{-1} after thermal treatment of the cell.

A DSC study was performed after charging the cells to 4.4 V to evaluate the effect of the Al$_2$O$_3$ coating on the thermal stability of the charged cathode. The heating rate was 3° C min^{-1}. The characteristic sharp exothermic peak is observed for bare LiCoO$_2$ at 263 °C see Fig. 11. For an Al$_2$O$_3$ coating, this peak shifts to higher temperature at 280 °C. At
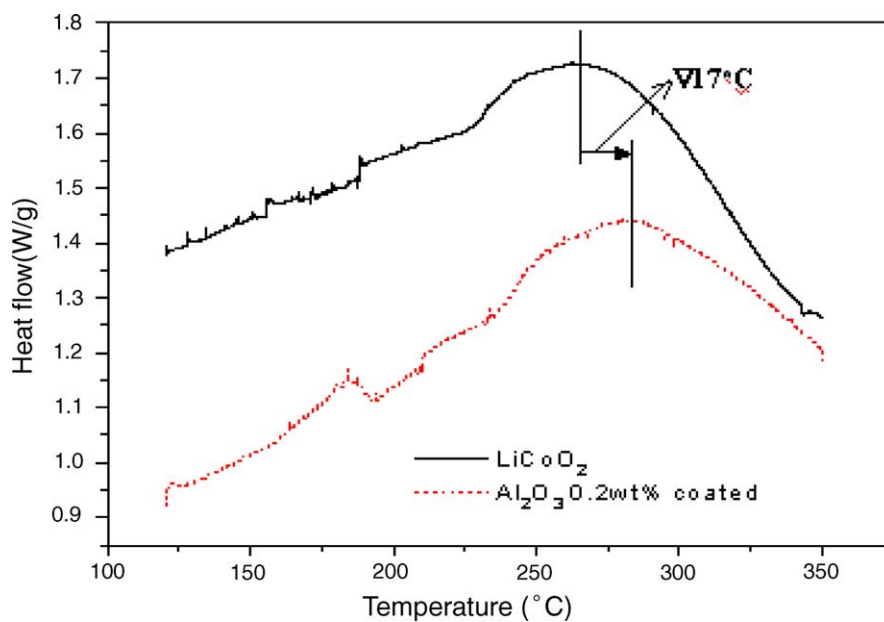
Fig. 11. DSC curves of charged cathodes containing bare and Al_2O_3-coated $LiCoO_2$. Cells charged to 4.4 V at 0.2 °C rate, equilibrated for 20 h at 4.4 V.

the same time, the area under the peak is decreased, which indicates that the extent of heat dissipation is decreased by employing an Al_2O_3 coating. Therefore, an Al_2O_3 coating is able to reduce the overall heat effect through better heat dissipation. Since Al_2O_3 is an excellent thermal conductor and the surface area of $LiCoO_2$ is increased by an Al_2O_3 coating, it can be concluded that the coating assists heat dissipation [20].

4. Conclusions

$LiCoO_2$ particles that are commercially employed as a cathode active material for lithium secondary batteries have been coated with Al_2O_3 by a gas-suspension spray coating method. It is found that theAl_2O_3 coating increases both the surface area and the electrical conductivity of $LiCoO_2$ particles. The distance of diffusion of Al^{3+} ions into the $LiCoO_2$ is about 15 nm and causes the formation of a thin layer of Li–Al–Co–O. Atomic absorption spectrophotometeric studies shows that the dissolution of Co from the Al_2O_3-coated $LiCoO_2$ in the electrolyte (1 M $LiPF_6$ dissolved in EC:DMC:EMC(1:1:1, vol.%) is lower than that of bare $LiCoO_2$. This can be attributed to the existence of a thin layer of Li–Al–Co–O, which protects the structure of the $LiCoO_2$ shell from the electrolyte.

The effect of Al_2O_3 coating on discharge capacity at various coating amounts is vary small on the first cycle, while it improves the capacity retention and thermal stability. This influence of Al_2O_3 can be explained by the fact that the Al_2O_3 layer on $LiCoO_2$ acts as an excellent thermal conductor as well as an electrical conductor. On the other hand, an excessive coating of Al_2O_3 degrades capacity retention on cycling due to a twist in the $LiCoO_2$ structure. In the experimental range used in this study, the Al_2O_3 coating that exhibits the highest capacity retention is 0.2 wt.% which correspond to a surface coverage of 13.7%.

Acknowledgements

References

[1] J. Cho, G. Kim, Electrochem. Solid-State Lett. 2 (1999) 253–255.
[2] R. Koksbang, J. Barker, H. Shi, M.Y. Saidi, Solid State Ionics 84 (1996) 1.
[3] M. Broussely, P. Biensan, B. Simon, Electrochem. Acta 45 (1999) 3.
[4] G.G. Amatucci, J.M. Tarascon, L.C. Klein, J. Electrochem. Soc. 143 (1996) 1114–1123.
[5] Z. Wang, L. Liu, L. Chen, X. Huang, Solid State Ionics 148 (2002) 335–342.
[6] T. Ohzuku, A. Ueda, J. Electrochem. Soc. 141 (1994) 2972.
[7] J.N. Reimers, J.R. Daim, J. Electrochem. Soc. 139 (1992) 2091.
[8] L. Liu, Z. Wang, H. Li, L. Chen, X. Huang, Solid State Ionics 152-153 (2002) 341–346.
[9] M. Holzapfel, R. Schreiner, A. Ott, E1ectrochem. Acta 46 (2001) 1063.
[10] S.T. Nywig, N. Kumagai, S. Komaba, H.T. Chung, Solid State Ionics 139 (2001) 147.
[11] H. Tukamoto, A.R. West, J. Electrochem. Soc. 144 (1997) 3164.
[12] C. Julien, G.A. Nazri, A. Rougier, Solid State Ionics 135 (2000) 121.
[13] J. Cho, Y.J. Kim, B. Park, Chem. Mater. 12 (2000) 3788.
[14] H.J. Kweon, S.J. Kim, D.O. Park, J. Power Sources 88 (2000) 255.

[15] E. Endo, T. Yasuda, A. Kita, K. Yamaura, K. Sekai, J. Electrochem. Soc. 147 (2000) 1291.

[16] H.J. Kweon, D.G. Park, Electrochem. Solid State Lett. 3 (2000) 128–130.

[17] S.Y. Park, J.K. Lee, K-S. Yoo, W. Cho, Y. Baek, Carbon Sci. 4 (2003) 74–78.

[18] C.T. Lynth, Practical Handbook of Material Science, CRC Press, Boston, 1989, pp. 304–305.

[19] Z. Zheng, Z. Tang, Z. Zhang, W. Shen, Y. Lin, Solid State Ionics 148 (2002) 317–321.

[20] S. Madhavi, G.V. Subba Rao, B.V.R. Chowdari, S.F.Y. Li, J. Power Sources 93 (2001) 156–162.